



ELSEVIER

Atmospheric Research 62 (2002) 57–70

ATMOSPHERIC
RESEARCH

www.elsevier.com/locate/atmos

Enhancement of contact nucleation by scavenging of charged aerosol particles

Sachchida N. Tripathi*, R. Giles Harrison

Department of Meteorology, University of Reading, P.O. Box 243, Earley Gate, Reading RG6 6BB, UK

Received 2 October 2001; received in revised form 1 February 2002; accepted 1 February 2002

Abstract

The influence of interparticle electrical forces on the particle collection rates of charged water drops are investigated using a particle–droplet trajectory model. For the charge levels expected naturally on supercooled water drops and aerosol active as contact nuclei, the charge-enhanced collection efficiency leads to an increased capture of ice nuclei (IN), causing the freezing probability by contact nucleation to be increased over neutral collisions. The collection efficiency depends on the aerosol charge, but not on the sign or charge carried by water drops. A threefold increase in the collection efficiency is found for aerosols carrying up to 10 elementary charges, collecting submicron aerosol. Modest charges on aerosol particles (APs) arising from natural asymmetries in ion concentration are sufficient to increase collision rates with suitable freezing nuclei. © 2002 Elsevier Science B.V. All rights reserved.

Keywords: Ice nucleation; Contact nuclei; Aerosol electrification; Atmospheric electricity; Electrofreezing

1. Introduction

Electrically induced freezing has been discussed in the literature (Pruppacher, 1973; Dawson and Cardell, 1973; Tinsley and Deen, 1991; Beard, 1992; Pruppacher and Klett, 1997); however, the mechanisms discussed differ substantially and no quantitative theories exist to test against experiments (Harrison, 2000). Highly electrified aerosol par-

* Corresponding author. Present address: Atmospheric, Oceanic and Planetary Physics, Department of Physics, Clarendon Laboratory, University of Oxford, Oxford, UK OX1 3PU. Fax: +44-1865-272923.

E-mail address: tripathi@atm.ox.ac.uk (S.N. Tripathi).

ticles (APs) are directly formed in aircraft exhausts (Yu and Turco, 1997) and a range of new techniques for the necessary atmospheric electrical measurements are becoming available (Aplin and Harrison, 2001; Harrison, 2001). Atmospheric observations (e.g. Pudovkin and Veretenenko, 1995) suggest that sudden changes in ionisation are associated with variations in properties of ice clouds although no mechanism is proposed. It is known that the supply of ions is critical to diffusive charging of aerosol particles (APs) and water droplets (Clement and Harrison, 1992) and that scavenging of aerosol by cloud droplets can be enhanced by electrical forces (Grover and Beard, 1975; Grover et al., 1977). If the aerosol scavenged by supercooled droplets are also active as ice nuclei (IN) in the contact mode (Young, 1974), the aerosol electrification could have a direct effect on the freezing properties of the cloud (Tinsley et al., 2000). Numerical calculations of the electric image charge effects were performed by Tinsley et al. (2000) for the particle radii 0.1 to 1.0 μm , colliding with droplets of 18.6–106 μm . They found that collision efficiency increased by up to factor of 30 for aerosols carrying a relatively large 50 charges, compared with that for phoretic and Brownian effects with relative humidity in the range of 95–100%.

In addition, Hobbs and Rangno (1990) have suggested contact nucleation is enhanced by the high liquid water contents near cloud edges. This observation may be important for the electrical problem, as it is clear that low conductivity regions permit longer retention of charge on aerosol and water drops (Clement and Harrison, 1992). Any of the usual scavenging mechanisms (hydrodynamic collision, turbulent diffusion, Brownian diffusion, thermophoresis and diffusiophoresis and electrically enhanced collisions) for particle capture could, in principle, influence contact nucleation; however, it is the possibility of electrical feedbacks on climate (Harrison, 1997), which motivates the investigation here.

Concentrations of IN suitable for contact and condensation–freezing are reviewed by Vali et al. (1984), which emphasises that concentrations of contact and condensation–freezing nuclei are similar at $-15\text{ }^{\circ}\text{C}$ (1–2 per litre). The concentration of immersion–freezing and deposition ice nuclei are 10 and 20 times lower, respectively. Cooper (1980) measured the concentration of contact ice nuclei and found that it decreases from 100 to 5 per litre when temperature increases from -20 to $-10\text{ }^{\circ}\text{C}$. Cooper also found that the concentration for deposition and immersion ice nuclei were typically an order of magnitude lower than concentration for contact ice nuclei. Values of the number fraction of aerosol particles active as IN by all nucleation modes, f_{IN} , found as a function of temperature are given in Fig. 1 (Pruppacher and Klett, 1997). f_{IN} falls rapidly with increasing temperature, the precise details of which depend on the size and type of IN concerned. There is a pronounced temperature dependence of f_{IN} .

2. Calculations of electrified particle collection

To investigate the sensitivity of freezing probability to electrical effects, the AP collection efficiency of a charged cloud droplet is calculated, taking full account of inertial and electrical (coulomb and image) forces. Using theoretical estimates for aerosol charges, the change in collection efficiency and the implied change in freezing probability were

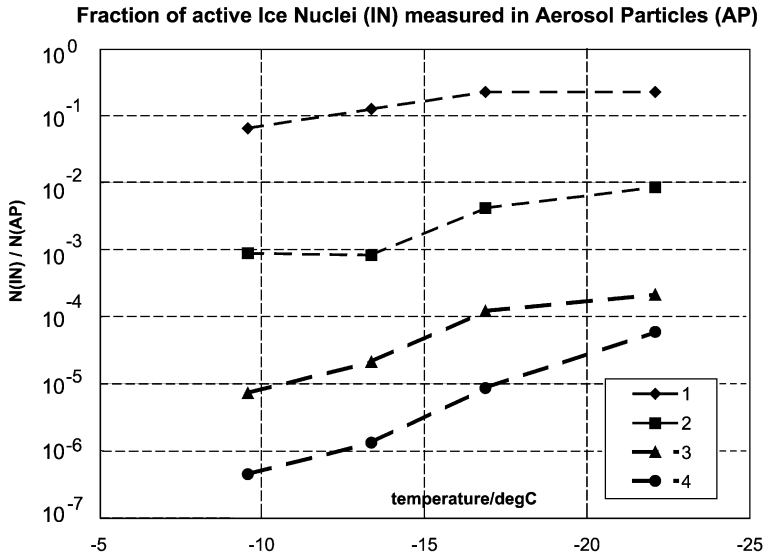


Fig. 1. Temperature dependence of the fraction of natural atmospheric aerosol particles active as ice nuclei by all freezing modes at water saturation, sampled from aircraft observations at Nalchik, U.S.S.R. Aerosol particles sizes (1) 100 μm , (2) 10 μm , (3) 1 μm , (4) 0.1 μm (Pruppacher and Klett, 1997).

deduced. This is compared with the change in freezing probability that could equally also be expected from a change in temperature.

2.1. Droplet scavenging model formulation

Previous particle collection calculations using the Coulomb force (Grover et al., 1977) and those including the electrical image force (Tinsley et al., 2000) have been applied to aerosol charges typical of the atmosphere in non-thunderstorm conditions (Tripathi, 2000). For aerosol particles of radii $a > 0.4 \mu\text{m}$, the collision efficiency, $E(A, a)$, between a drop of radius A and particle of radius a is determined by integrating the equation of motion of an aerosol particle under the simultaneous influences of gravity, air drag, and electrical forces. Formally, the collision efficiency, E is defined as:

$$E(A, a) = \frac{\pi y_c^2}{\pi(A + a)^2}, \quad (1)$$

where A is the drop radius, a particle radius, and y_c the largest horizontal offset which a particle can have from the drop axis, yet still collide with it (Pruppacher and Klett, 1997). The collection efficiency is computed from an analysis of the trajectory of the aerosol particles moving past the water drop, assuming the flow around the aerosol particle does not affect the drop motion. This is justified for a ratio of particle to collector drop masses less than 10^{-3} .

The equation of motion of the aerosol is:

$$m \frac{d\mathbf{V}}{dt} = mg^* - \frac{6\pi\eta A(\mathbf{V} - \mathbf{U})}{1 + \alpha N_{Kn}} + \mathbf{F}_e, \quad (2)$$

where m , \mathbf{V} and a are the mass, velocity, and radius of the aerosol particle, respectively, (Grover and Beard, 1975) and $(1 + \alpha N_{Kn})$ is the Stokes–Cunningham slip correction factor required for the aerosol particles. (Vector quantities are in boldface type.) In Eq. (2), $g^* = g(\rho_p - \rho_a)/\rho_p$, where g is the acceleration due to gravity, ρ_p the density of the aerosol particle, ρ_a the density of the air, η the viscosity of air, \mathbf{U} the velocity of the air around collector drop, and \mathbf{F}_e the electric force between the water drop and aerosol. The Knudsen number is $N_{Kn}(= \lambda_a/a)$, where λ_a is the mean free path of air molecules. The parameter α is given by Junge (1963) as:

$$\alpha = 1.26 + 0.44\exp(1.07/N_{Kn}). \quad (3)$$

The particle's trajectory is obtained by numerically integrating Eq. (2) in the reference frame of the drop. From the trajectory, the collision efficiency may be calculated. To determine the local hydrodynamic velocity \mathbf{U} , it is necessary to evaluate the air drag (second term in the RHS of Eq. (2)). The flow fields outside a noncirculating water drop were computed by solving the complete Navier–Stokes equation of motion for steady incompressible flow past a rigid sphere using a method originally developed by LeClair et al. (1970). In the convective flow around the drop, the gradients of the stream function and vorticity are greatest close to the drop surface. Far from the surface, these gradients are small. Because of this, a nonuniform mesh system is used for the finite difference calculations. The drag coefficients obtained have been compared with those of LeClair et al. (1970) and Beard and Pruppacher (1969) for drop radii between 8 and 140 μm (Tripathi, 2000). They are always within 5% of the earlier numerical and experimental values (Table 1).

The particle's equation of motion expressed by Eq. (2) can be written as:

$$\frac{d\mathbf{V}}{dt} = \frac{\hat{\mathbf{z}}}{N_{Fr}} - \frac{1}{S_t}(\mathbf{V} - \mathbf{U}) - \frac{\mathbf{F}_e}{mg^*N_{Fr}}, \quad (4)$$

with $\hat{\mathbf{z}}$ the unit vector in the vertical direction. This can be made dimensionless by substitution of:

$$t = \frac{t' U_\infty}{A}, \quad (5)$$

$$\mathbf{V} = \frac{\mathbf{V}'}{U_\infty}, \quad (6)$$

$$\mathbf{U} = \frac{\mathbf{U}'}{U_\infty}, \quad (7)$$

Table 1

Comparison of drag coefficients, C_D , obtained with those of LeClair et al. (1970) and Beard and Pruppacher (1969), for drop radii between 8 and 140 μm

N_{Re}	C_D (present results)	$C_D N_{\text{Re}}^2$ (present results)	C_D (theoretical results; LeClair et al., 1970)	$C_D N_{\text{Re}}^2$ (experimental results; Beard and Pruppacher, 1969)	Percentage difference in C_D	Percentage difference in $C_D N_{\text{Re}}^2$
0.01	2425	0.242	2446.69	–	– 0.86	–
0.1	242.5	2.42	246.22	2.427	– 1.53	– 0.28
0.2	121.6	4.86	–	4.90	–	– 0.82
0.3	80.84	7.27	–	7.43	–	– 2.20
0.5	48.5	12.12	–	12.63	–	– 4.20
1	27.04	27.04	27.39	26.448	– 1.29	2.18
2	13.78	55.12	–	57.49	–	– 4.29
3	10.09	90.81	–	91.98	–	– 1.28
4	8.12	129.9	–	129.56	–	0.26
5	6.89	172.25	7.121	170.171	– 3.35	1.20
7	5.41	264.6	–	259.99	–	1.74
9	4.55	368.55	–	360.69	–	2.13
10	4.23	423.67	4.337	414.94	– 2.52	2.05
20	2.69	1079.6	2.73	1090.04	– 1.48	– 1.01

N_{Re} is the Reynolds number.

where A is drop radius, U_∞ the terminal velocity of the droplet, the Stokes number $St = (2U_\infty \rho_p a^2 (1 - \alpha N_{\text{Kn}})) / 9\eta A$ and the Froude number $N_{\text{Fr}} = U_\infty^2 / g * A$ (Grover and Beard, 1975). The primed quantities represent the dimensionless versions of the variables, which are used in the numerical calculations only.

2.2. Electrical image forces

Fig. 2 illustrates the relevant aerosol–droplet geometry. The electrical forces always act along the line between the centres of the aerosol and drop, when the aerosol is taken as a point charge and the drop is taken to be a conducting sphere. This is a good approximation even for distilled water, which has a very short electrical relaxation time, 10^{-4} s (MacGorman and Rust, 1998). A dielectric sphere behaves much like a pure conductor once the dielectric constant, κ , is >80 (Grover, 1976).

In Fig. 2, the drop carries a net charge Q_d and the aerosol particle a net charge Q_a with a distance s between the aerosol and drop centres. It can be shown that the particle charge causes the charge on the conducting sphere to redistribute itself, equivalent to two point charges (Jackson, 1975). Charge conservation requires that $Q_d = I + D$. In magnitude, $I = -(A/s)Q_a$, where s is the separation distance between the aerosol and drop centres. The image charge is located at a distance c from the centre of the drop. Summing the Coulomb and image forces, the net electrical force acting between the particles' centres is therefore:

$$F_e = \frac{1}{4\pi\epsilon_0} \left[\frac{Q_a I}{(s - c)^2} + \frac{Q_a D}{s^2} \right], \quad (8)$$

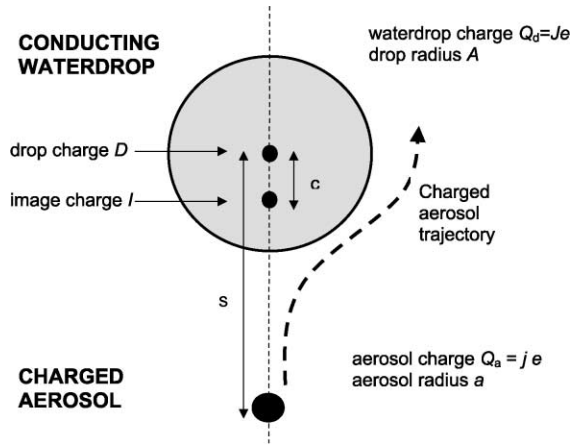


Fig. 2. Schematic of the charged aerosol and image charge construction within a waterdrop of radius A . The aerosol and falling drop carry charges, Q_a and Q_d , respectively, with $Q_d = I + D$, where D is the non-image charge considered at the centre of the drop.

where a positive F_c is repulsive. Substituting for Q_a , Q_d and c gives:

$$F_c = L \left[-\frac{r}{(r^2 - 1)^2} + \frac{1}{r^3} (Kr + 1) \right], \tag{9}$$

where $r = s/A$ is the normalised distance between the particle and drop, $K = Q_d/Q_a$ and $L = j^2 e^2 / 4\pi\epsilon_0 A^2$ (Tinsley et al., 2000). ϵ_0 is the permittivity of free space. F_c can be substituted for the Coulomb force in the Eq. (4), such that $\mathbf{F}_c = F_c \hat{\mathbf{r}}$.

$$\frac{d\mathbf{V}}{dt} = \frac{\hat{\mathbf{z}}}{N_{Fr}} - \frac{1}{S_t} (\mathbf{V} - \mathbf{U}) - \frac{F_c}{mg^*} \frac{\hat{\mathbf{r}}}{N_{Fr}}, \tag{10}$$

where $\hat{\mathbf{r}}$ is the unit vector along the line joining the centres of aerosol and drop.

Eq. (10) was integrated using the fifth order Runge–Kutta method to obtain collision efficiencies for different sets of drops ($18 \leq A \leq 70 \mu\text{m}$) and aerosols ($0.1 \leq a \leq 4 \mu\text{m}$). The value of largest horizontal offset between droplet and aerosol y_c was found by choosing an initial offset value ($2.5A$), and integrating the resulting trajectory in time. For subsequent trajectories, the offset was determined by bisecting the previous offset value until a grazing collision occurs, when $(y_{i+1} - y_i)/y_i < \epsilon_c$, where ϵ_c is the collision tolerance. For such a grazing collision, $y_c = y_{i+1}$. The collision tolerance was chosen as $\epsilon_c = 10^{-4}$ (e.g. Miller and Wang, 1989). The initial aerosol–droplet vertical separation was $16A$ (Tripathi and Harrison, 2001), with no substantial change in the collision efficiency found by reducing the distance.

2.3. Collision efficiency results

In Fig. 3(a), the collision efficiency is plotted as a function of aerosol radius with both the Coulomb and image forces included for particle density, $\rho_p = 2 \text{ g cm}^{-3}$. For the neutral aerosols, inertial forces are not important for particles with radii smaller than about $2.8 \mu\text{m}$. The ‘Greenfield Gap’ (Pruppacher and Klett, 1997) can also be seen for particles of radii between 1.2 and $2.8 \mu\text{m}$. For particles with radii larger than $3 \mu\text{m}$, inertial effects become very important and the collision efficiency rises sharply. Fig. 3(a) also shows that the effect of electrification is most pronounced for aerosols with radii $a < 1 \mu\text{m}$, for which electrified aerosols have substantially greater collision efficiencies than neutral aerosols. A mean charge of 10 electronic charges per particle is sufficient to increase the collision efficiency threefold over that for neutral particles. At larger radii, $a > 1 \mu\text{m}$, there is little effect and the electrical forces are swamped by the inertial forces and it requires more than about $200e$ charges to fill the Greenfield Gap.

In Fig. 3(a), the results of Grover and Beard (1975) (inertial and image forces) and Tinsley et al. (2000) (image force) are included for comparison with the present results.

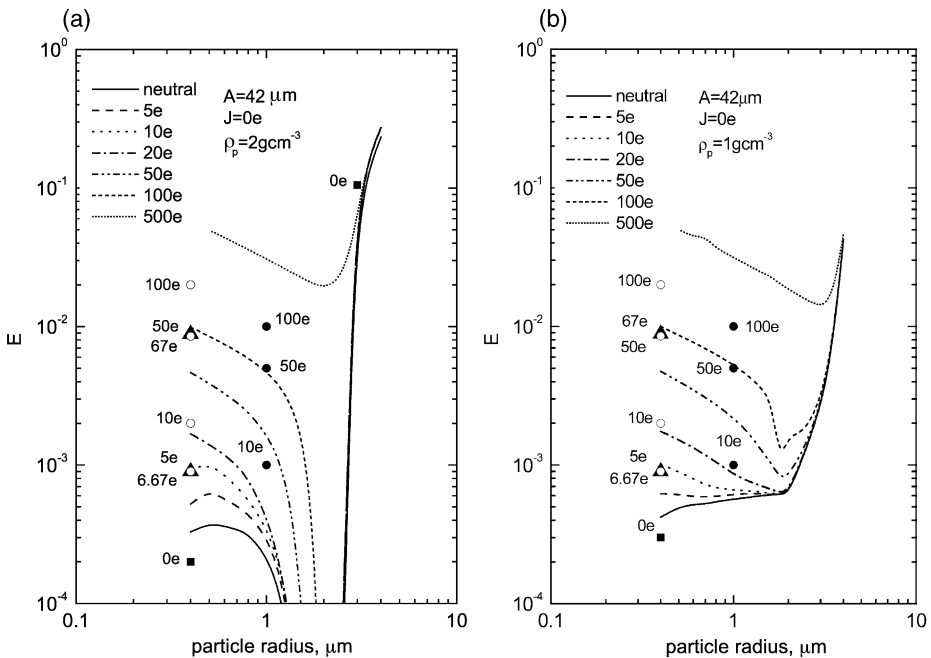


Fig. 3. (a) Collision efficiencies E plotted as a function of aerosol radius for aerosol particles carrying charges, $5e$ to $50e$, for aerosol density, $\rho_p = 2 \text{ g cm}^{-3}$. The droplet radius is constant at $42 \mu\text{m}$ and is electrically neutral. (\blacksquare : Inertial collision efficiencies, E , by Grover et al., 1977 for aerosol radii 0.4 and $3.0 \mu\text{m}$, respectively. \blacktriangle : Image force calculations by Grover and Beard, 1975 for particle of radius $0.4 \mu\text{m}$ having charges $6.7e$ and $67e$, respectively. \circ : Image force calculations by Tinsley et al., 2000 for particle of radius $0.4 \mu\text{m}$ having charges $5e$, $10e$, $50e$ and $100e$, respectively. \bullet : Image force calculations by Tinsley et al., 2000 for particle of radius $1.0 \mu\text{m}$ having charges $6.7e$ and $67e$.) (b) As (a) except for $\rho_p = 1 \text{ g cm}^{-3}$.

Comparing the inertial collision efficiencies with those of Grover and Beard (1975) (squares), it can be seen that difference is about 50% for 0.4- μm -radius particle, but reduces to less than 5% for a 3.0- μm -radius particle. In the absence of electrical forces, the flow field becomes important because it provides the only non-zero forcing term. The flow fields are calculated here using much finer grid sizes, especially in the near neighbourhood of the drop. Comparing the image force calculations with Grover and Beard (1975) (triangles), less than 25% difference is found for 0.4- μm particle having 6.7 and 67 elementary charges. This could be due to the fact that Grover and Beard (1975) used electrical image force assuming both particles (aerosol and droplet) as two spheres and the resulting electrical force provides the maximum attractive force. In the present calculations, the electrical image force arises from conducting sphere and point charge representations of droplet and aerosol, respectively; thus, the second and higher order moments do not appear.

Differences up to factor of two are found between this work and those of Tinsley et al. (2000) for 0.4- μm -radius particles (open circles) and increases for particles of radius 1 μm (filled circles). Tinsley et al. (2000) neglected inertial forces, considering the aerosol as a point with the image force the principal force. Tinsley et al. (2000) also simplified the flow field around the droplet by assuming Stokes flow. This assumption leads to smaller drag forces, which will, in turn, result in slightly larger collision efficiencies. The effect of gravitational forces is emphasised by the calculations presented in Fig. 3(b), for a particle density of 1 g cm^{-3} . Comparing Fig. 3(a) and (b), the difference between the present calculations and those performed by Grover and Beard (1975) and Tinsley et al. (2000) decreases because smaller gravitational forces act on the particles of lower density.

In Fig. 4, collision efficiency is plotted as a function of aerosol radius for a 52- μm droplet. Narrowing of the Greenfield Gap can be seen due to increased drag forces; ~ 50 electronic charges is required on the aerosol particles to remove the gap. Comparing Figs. 3(a) and 4(a) and (b), the charged collision efficiency increases with decreasing droplet radius because of increasing significance of electrical forces over drag forces. A similar trend was also noticed by Tinsley et al. (2000).

Referring back to Fig. 1, the fraction of aerosol active across all freezing modes is small for the small radii (curve 4) showing the steepest temperature dependence. The assumption is made here that electrical enhancement of the collection of contact nuclei is equivalent to the increase the freezing nuclei fraction occurring from a temperature reduction. This permits electrical changes in collision efficiency to be compared with changes in temperature.

2.4. Particle charges

To establish if there is likely to be any effect on natural supercooled clouds from electrification of submicron aerosol, it is necessary to estimate what charges can be expected on atmospheric particles. Particle charges can be calculated assuming charging by ion diffusion for the small electrical fields present in nonconvective clouds. Electric field measurements in non-thunderstorm clouds are less than 5 kV m^{-1} and typically less than 1 kV m^{-1} (MacGorman and Rust, 1998). The number concentration N_j of mono-

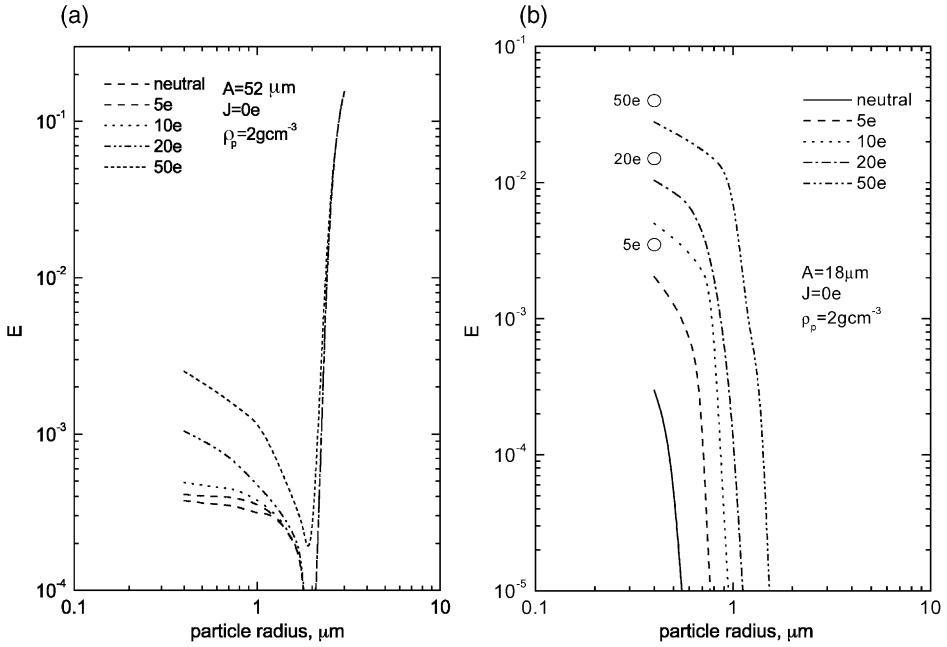


Fig. 4. (a) Collision efficiencies E plotted as a function of particle radius for droplet of radius $52 \mu\text{m}$. All other parameters are same as in Fig. 3(a). (b) Collision efficiencies E plotted as a function of particle radius for droplet of radius $18 \mu\text{m}$. All other parameters are same as in Fig. 3(a). (O: Image force calculations by Tinsley et al. (2000) for particles of radius $0.4 \mu\text{m}$ having charges $5e$, $20e$ and $50e$, respectively).

disperse aerosol particles per unit volume carrying j elementary charges is given by the Modified Boltzmann Distribution (Clement and Harrison, 1992) as:

$$\frac{N_j}{N_0} = \left[\frac{n_+ \mu_+}{n_- \mu_-} \right]^j \frac{8\pi\epsilon_0 akT}{je^2} \sinh \left[\frac{je^2}{8\pi\epsilon_0 akT} \right] \exp \left[\frac{-j^2 e^2}{8\pi\epsilon_0 akT} \right], \quad (11)$$

with mean charge:

$$j = \frac{4\pi\epsilon_0 akT}{e^2} \ln \left[\frac{n_+ \mu_+}{n_- \mu_-} \right], \quad (12)$$

where μ_{\pm} are the positive and negative small ion mobilities and n_{\pm} their number concentrations, T is the temperature, e the electronic charge, k is Boltzmann's constant, and ϵ_0 the permittivity of free space. Ion mobility is defined as the ion drift velocity in a unit electric field and has units of $\text{cm}^2 \text{V}^{-1} \text{s}^{-1}$.

The ion asymmetry factor $x(= \mu_+ n_+ / \mu_- n_-)$ determines the mean of the charge distribution. $x \neq 1$ for two reasons:

1. chemical differences between positive and negative ions cause $\mu_+ \neq \mu_-$, which arise from different polarising powers of the central atom in positive and negative ions, and a different molecular mass.

2. $n_+ \neq n_-$ because the ion concentrations n_+ and n_- vary considerably in the atmosphere, especially on the boundaries of aerosol and water droplet regions (Gringel, 1978).

Continuous mountain recordings of n_+ and n_- have been carried out by Reiter (1974) and Dolezalek et al. (1985), and the ratio of ion concentrations varies substantially with weather conditions (Table 2). Because of the probabilistic nature of the charging process of aerosol particles, a few particles could also transiently carry higher charges (Harrison, 2000); however, their lifetimes are not experimentally established. The fraction of particles carrying large charges increases for $x \gg 1$ or $x \ll 1$.

Charge distributions on particles can also be expressed as a number of particles carrying a certain charge in a prescribed total monodisperse aerosol concentration. In Fig. 5, the number of concentrations of particles of various radii from 3 to 0.5 μm carrying specified bipolar charges, normalised by the total number per unit volume Z , are plotted as a function of ion asymmetry factor x for the number of elementary charges $j=10$ and 20, using Eq. (11). The straight line marked indicates the region above which is at least 1 particle/ cm^3 carrying charges $>|j|$ will be present with $Z=1000 \text{ cm}^3$. From Fig. 5(a), it is clear that for particles of 0.5- μm radius, only a very insignificant fraction will carry more than ± 20 charges; however, Fig. 5(b) shows that there will be some particles present carrying more than ± 10 charges.

Taken together, these observations suggest that (1) some charged aerosol particles *always* exist in the atmosphere and (2) fluctuations in ion concentrations causing $x \neq 1$ could lead to larger charges on aerosols, perhaps on cloud edges or aerosol boundaries.

3. Freezing probabilities

For the purpose of calculating the electrically induced changes in aerosol collection, an enhancement factor P is defined here as:

$$P = E(a, j, A, J) / E_{\text{neutral}}, \quad (13)$$

where E is the droplet's efficiency in collecting aerosol particles, which varies with the particle radius a and the number of charges j , and A and J the droplet's radius and the

Table 2
Values of ion asymmetry factor x reported by Reiter (1977) in different conditions

Cloud	Weather condition	Altitude (km)	Ion asymmetry factor x
Mountain clouds	Fair weather	0.74	1.75–2.5
Nimbostratus	Homogeneous steady rain	1–1.8	2.5
		1.8–3	10–20
	Steady snow fall	1.–1.6	3.2
Altostratus	Weak precipitation	1.6–3	4–5
		1–1.4	4–30
		1.4–3	2–10

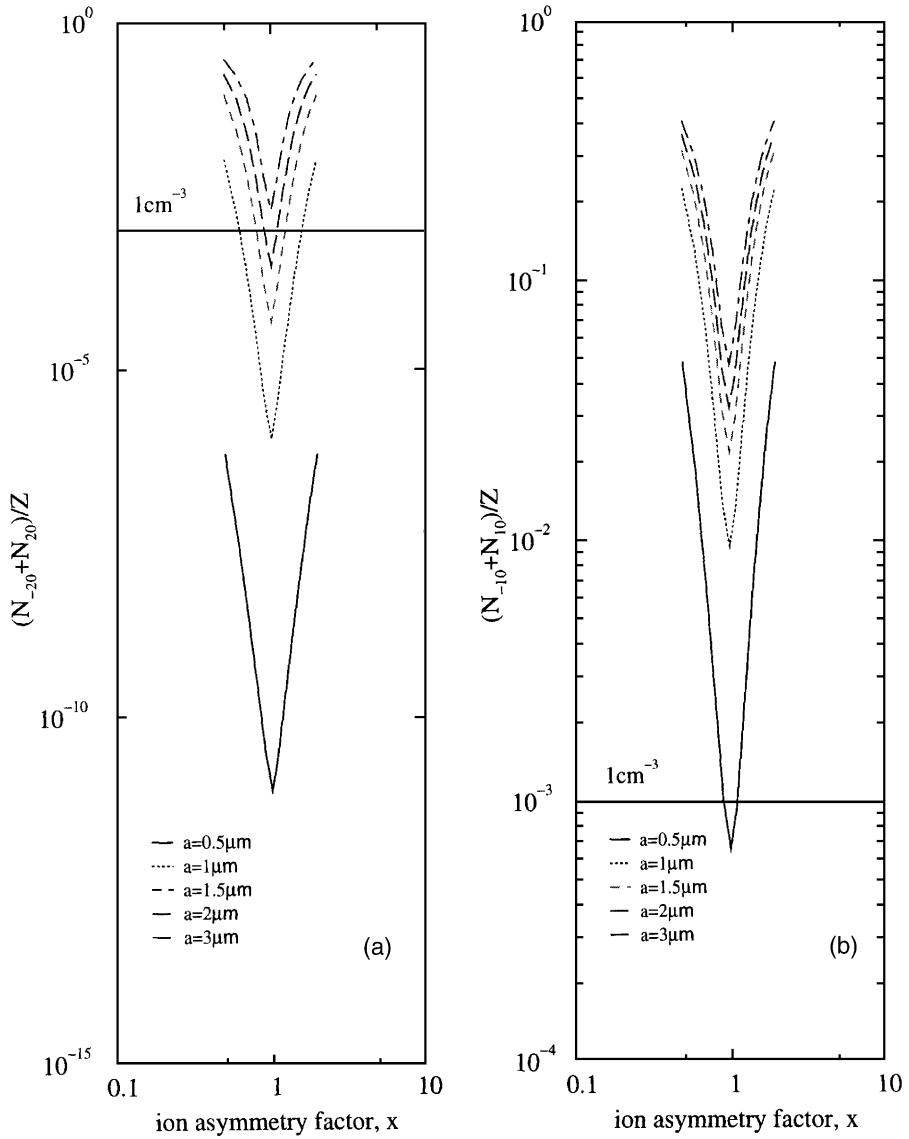


Fig. 5. (a) The fraction of aerosol particles carrying -20 and $+20$ electronic charges $(N_{20} + N_{-20})/Z$, plotted as a function of ion asymmetry factor x for various aerosol radii a . The horizontal line indicates the region above which a concentration of $1 \text{ particle cm}^{-3}$ will be present, for total number concentration $Z = 10^3 \text{ cm}^{-3}$. (b) As (a) except calculated for N_{-10} and N_{+10} .

number of charges. E_{neutral} is the droplet collision efficiency for electrically neutral aerosol particles.

In Fig. 6, the electrical enhancement P is shown for three cloud droplets of radius 40 , 32 and $26 \mu\text{m}$ for charged collisions for three aerosol particles of radii $a = 0.4 \mu\text{m}$, 0.5 and

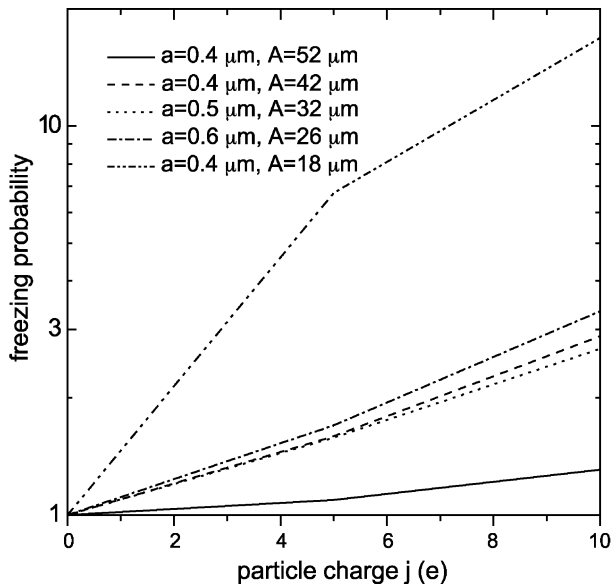


Fig. 6. Freezing probability from electrical enhancement of aerosol collection rate P , calculated as a function of particle elementary charges j . Neutral (supercooled) droplets of radii 52, 40, 32, 26 and 18 μm are considered to collect charged aerosol particles of radii 0.4, 0.4, 0.5, 0.6 and 0.4 μm , respectively.

0.6 μm , respectively. Three radii have been selected to optimise the electrical effect over inertial effects as found from Fig. 3, but are representative of some atmospheric IN. The maximum numbers of drops are frequently found near radii of $\sim 20\text{--}30 \mu\text{m}$ in a typical cloud droplet spectrum (Hobbs et al., 1980).

Comparing the curves in Fig. 6 shows that electrical effects become more significant as the drop size decreases. It can also be seen that for a drop size of 26 μm , the freezing probability is increased by a factor of three for a particle carrying 10 e . From Fig. 1, approximately a threefold fractional increase in active nuclei can be seen for a temperature decrease of 1 $^{\circ}\text{C}$. Hence, to order of magnitude, the change in collected ice nuclei arising from a temperature decrease of 1 $^{\circ}\text{C}$ is approximately comparable with that produced by a change in particle charge of $\sim |10e|$.

4. Conclusions

Collection efficiency calculations applied to the collection of charged aerosols show that modest charging of submicron radii aerosols can lead to more collisions with supercooled droplets than neutral aerosol, a fraction of which will be associated with ice nucleation. The change in collision rate occurs from the electrical image force and is, therefore, independent of the charge carried by the water drop. The aerosol charging arises from asymmetry in ion concentrations associated with electric field discontinuities such as on the boundaries of clouds. Sufficient ion asymmetry occurs naturally for a distribution of

aerosol charges to occur, and a small number fraction of aerosol can, therefore, carry up to 10 elementary charges. For an aerosol population containing a constant fraction of contact nuclei, the droplet's freezing probability can be enhanced by the electrical collection. This is particularly so in the case of small ($<20\ \mu\text{m}$) supercooled droplets, or for the few aerosol particles which statistically may transiently carry large charges.

There are recent developments in high spatial resolution atmospheric electrical measurements; however, definitive experimental studies firmly linking electrified aerosol and freezing remain lacking. More atmospheric and laboratory work is clearly required; however, theoretical evidence here supports the few experiments suggesting electrical effects on ice formation in low electric fields.

Acknowledgement

SNT acknowledges financial support from the Felix Foundation.

References

- Aplin, K.L., Harrison, R.G., 2001. A self-calibrating programmable mobility spectrometer for atmospheric ion measurements. *Rev. Sci. Instrum.* 72 (8), 3467–3469.
- Beard, K.V., 1992. Ice initiation in warm-base convective clouds: an assessment of microphysical mechanisms. *Atmos. Res.* 28, 125–152.
- Beard, K.V., Pruppacher, H.R., 1969. A determination of the terminal velocity and drag of small water drops by means of a wind tunnel. *J. Atmos. Sci.* 26, 1066–1072.
- Clement, C.F., Harrison, R.G., 1992. The charging of radioactive aerosols. *J. Aerosol. Sci.* 24, 481–504.
- Cooper, W.A., 1980. A method of detecting contact ice nuclei using filter samples. 8th Int. Conf. Cloud Phys. Am. Meteor. Soc., Boston, pp. 667–668.
- Dawson, G.A., Cardell, G.R., 1973. Electrofreezing of supercooled waterdrops. *J. Geophys. Res.* 78 (36), 8864–8866.
- Dolezalek, H., Reiter, R., Kroling, R., 1985. Basic comments on the physics, occurrence in the atmosphere, and possible biological effects of air ions. *Int. J. Biometeorol.* 29, 207–242.
- Gringel, W., 1978. Untersuchungen zur elektrischen Luftleitfähigkeit unter Berücksichtigung der Sonnenaktivität und der Aerosolteilchenkonzentration bis 35 km Höhe, PhD dissertation, Eberhard-Karls-Universität zu Tübingen.
- Grover, S.N., 1976. Electrostatic force between a charged conducting sphere and a charged dielectric sphere in an arbitrarily oriented external electric field. *Pure Appl. Geophys.* 114, 520–539.
- Grover, S.N., Beard, K.V., 1975. A numerical determination of the efficiency with which electrically charged cloud drops and small raindrops collide with electrically charged spherical particles of various densities. *J. Atmos. Sci.* 32, 2156–2165.
- Grover, S.N., Pruppacher, H.R., Hamielec, A.E., 1977. A numerical determination of the efficiency with which spherical aerosol particles collide with spherical water drops due to inertial impaction and phoretic and electrical forces. *J. Atmos. Sci.* 34, 1655–1663.
- Harrison, R.G., 1997. Climate change and the global atmospheric electrical system. *Atmos. Environ.* 31 (20), 3483–3484.
- Harrison, R.G., 2000. Cloud formation and the possible significance of charge for atmospheric condensation and ice nuclei. *Space Sci. Rev.* 94, 381–396.
- Harrison, R.G., 2001. A balloon-carried electrometer for high-resolution atmospheric electric field measurements in clouds. *Rev. Sci. Instrum.* 72 (6), 2738–2741.
- Hobbs, P.V., Rangno, A.L., 1990. Rapid development of high particle concentrations in small polar maritime cumulus clouds. *J. Atmos. Sci.* 47, 2710–2722.

- Hobbs, P.V., Politovich, M.K., Radke, L.F., 1980. The structure of summer convective clouds in eastern Montana I: natural clouds. *J. Appl. Meteorol.* 19, 645–663.
- Jackson, J.D., 1975. *Classical Electrodynamics*, Wiley, New York.
- Junge, C.E., 1963. *Air Chemistry and Radioactivity*, New York, Academic Press.
- LeClair, B.P., Hamielec, A.E., Pruppacher, H.R., 1970. A numerical study of the drag on a sphere at low and intermediate Reynolds numbers. *J. Atmos. Sci.* 27, 308–315.
- MacGorman, D.R., Rust, W.D., 1998. *The Electrical Nature of Storms*, Oxford Univ. Press, Oxford.
- Miller, N.L., Wang, P.K., 1989. Theoretical determination of the efficiency of aerosol particle collection by falling columnar ice crystals. *J. Atmos. Sci.* 46 (12), 1656–1663.
- Pruppacher, H.R., 1973. Electrofreezing of supercooled water. *Pure Appl. Geophys.* 104, 623–634.
- Pruppacher, H.R., Klett, J.D., 1997. *Microphysics of Clouds and Precipitation*, 2nd edn. Kluwer Academic Publishing, Dordrecht.
- Pudovkin, M.I., Veretenenko, S.V., 1995. Cloudiness decreases associated with Forbush-decreases of galactic cosmic rays. *J. Atmos. Terr. Phys.* 75, 1349–1355.
- Reiter, R., 1977. Atmospheric electricity activities of the institute for atmospheric environmental research. In: Dolezalek, H., Reiter, R. (Eds.), *Electrical Processes in Atmospheres*. Steinkopff Verlag, Darmstadt, pp. 759–796.
- Tinsley, B.A., Deen, G.W., 1991. Apparent tropospheric response to MeV–GeV particle flux variations: a connection via electrofreezing of supercooled water in high-level clouds? *J. Geophys. Res.* 96, 22283–22296.
- Tinsley, B.A., Rohrbaugh, R.P., Hei, M., Beard, K.V., 2000. Effects of image charges on the scavenging of aerosol particles by cloud droplets, and on droplet charging and possible ice nucleation processes. *J. Atmos. Sci.* 57, 2118–2134.
- Tripathi, S.N., 2000. Removal of charged aerosols, PhD thesis, The University of Reading, UK.
- Tripathi, S.N., Harrison, R.G., 2001. Scavenging of electrified radioactive aerosols. *Atmos. Environ.* 35 (33), 5817–5821.
- Vali, G., Deshler, T., Rogers, D.C., 1984. Concentration of ice nuclei of different modes of activation. 11th Int. Conf. Atmos. Aerosols, Conde. Ice Nuclei, Hungarian Meteorol. Serv., Budapest, Hungary, vol. 2, pp. 105–109.
- Young, K.C., 1974. The role of contact nucleation in ice phase initiation in clouds. *J. Atmos. Sci.* 31, 768–776.
- Yu, F., Turco, R., 1997. The role of ions in the formation and evolution of particles in aircraft plumes. *Geophys. Res. Lett.* 24, 1927–1930.